EFDA–JET–PR(14)20

I.E. Stamatelatos, T. Vasilopoulou, P. Batistoni, S. Conroy, B. Obryk,
S. Popovichev, D.B. Syme and JET EFDA contributors

Neutron Streaming Through the JET Personnel Entrance Labyrinth

Neutron Streaming Through the JET Personnel Entrance Labyrinth

I.E. Stamatelatos[1], T. Vasilopoulou[1], P. Batistoni[2,3], S. Conroy[2,4], B. Obryk[5], S. Popovichev[2], D.B. Syme[2] and JET EFDA contributors*

JET-EFDA, Culham Science Centre, OX14 3DB, Abingdon, UK

[1]Institute of Nuclear and Radiological Sciences, Technology, Energy & Safety, NCSR "Demokritos", Athens, Greece,
2EFDA JET, Culham Science Centre, OX14 3DB, Abingdon, OXON, UK
[3]ENEA, Frascati, Rome, Italy,
[4]Department of Physics and Astronomy, Uppsala University, Uppsala, Sweden
[5]Henryk Niewodniczański Institute of Nuclear Physics of the Polish Academy of Sciences, Kraków, Poland
** See annex of F. Romanelli et al, "Overview of JET Results",*
(24th IAEA Fusion Energy Conference, San Diego, USA (2012)).

Preprint of Paper to be submitted for publication in
Applied Radiation and Isotopes

ABSTRACT

Neutron streaming through the personnel entrance labyrinth of the Joint European Torus (JET) Hall was evaluated. Monte Carlo calculations using the MCNP code were performed in order to predict neutron fluence and ambient dose equivalent along the labyrinth. The calculations were validated by comparison with measurements performed using thermoluminescence detectors. Simulations were performed for both D-D and D-T toroidal plasma discharge sources. Baseline calculations were performed for the "as-built" concrete composition. The sensitivity of the calculations on hydrogen and boron content in concrete was examined. The results of the study showed that neutron streaming through the labyrinth is independent of the initial energy of the plasma source and depends only on the labyrinth geometry and material configuration. The present work supports the operational radiation protection effort to minimize collective radiation dose to personnel at JET. Moreover it provides important information from JET experience that may assist in the optimization and validation of the radiation shielding design methodology used for ITER.

1. INTRODUCTION

The Joint European Torus (JET) is currently the largest tokamak in the world. The experiments and design studies performed by JET are consolidated to a large extent into the design of its successor ITER and the demonstration fusion reactor DEMO. Among others, experiments are being carried out at JET aiming to validate in a real fusion environment the neutronic codes and nuclear data applied in ITER nuclear analyses (Batistoni et al., 2014). In particular, measurements and calculations of the neutron fluence through the penetrations of the JET shielding walls aim to assess the capability of numerical tools to accurately predict neutron transport along the long paths and the complex geometries characterizing the ITER biological shield.

In the present work, neutron streaming through the JET Hall South West personnel entrance labyrinth was evaluated. Monte Carlo calculations using the MCNP code were performed in order to predict neutron fluence and ambient dose equivalent. Deuterium-Deuterium (D-D) and Deuterium-Tritium (D-T) toroidal plasma discharge sources were simulated. Baseline calculations were performed for the "as-built" concrete walls composition. Moreover, the sensitivity of the calculations on hydrogen and boron content in concrete was examined. The results of the calculations were validated by comparison against measurements carried out by Obryk et al (2014a, 2014b) using thermoluminesance detectors.

2. SIMULATIONS METHODOLOGY

Simulations were performed using Monte Carlo code MCNP-X (version 2.5.0) (McKinney et al., 2006). Cross-section data were obtained from JEFF 3.1.2 (Santamarina et al. 2009) and FENDL 2.1 (Aldama et al., 2004) libraries. Simulations were performed for D-D and D-T toroidal plasma sources.

2.1 GEOMETRY AND MATERIALS

The personnel entrance labyrinth is located at the South West (SW) corner of the JET Hall (Fig. 1). The geometry and dimensions of the labyrinth are shown in Fig.2. The labyrinth configuration provides four right-angle turns. The total length of the labyrinth is 11.80 m and its height is 2.60m. The labyrinth width varies between 0.90 and 1.10m and therefore the labyrinth cross-sectional area ranges between 2.34m^2 and 2.86 m^2. The thickness of the concrete wall is 2.50m. The internal surface of the Hall wall is covered by a layer of borated concrete (0.30 m in thickness). The densities of concrete and borated concrete were 2.43×103kg·m^{-3} and 2.20×103 kg·m^{-3}, respectively. The "as-built" compositions of concrete and borated concrete are shown in Table 1.

Calculations were performed for the "as-built" concrete composition. Moreover, MCNP runs were performed to study the sensitivity of the calculations on changes in the hydrogen and boron content in concrete. Hydrogen content (by weight) in plain and borated concrete was altered from 0.41% to 0.71% and from 0.05% to 0.35%, respectively. Boron in borated concrete was altered from 0% to 5%. It is stressed that the density of plain and borated concrete was not changed in these runs and it was kept as in the "as-built" concrete composition.

2.2 CALCULATIONS DETAILS

A two-stage simulation approach was employed. A detailed model of the JET Torus (Gatu-Johnson et al., 2008) was used to produce a Surface Source Write file registering the neutrons directed towards the South West corner of the JET Hall. The model took into consideration the actual toroidal distribution of the neutrons produced in the JET plasma. The modeled geometry included the plasma facing components, the vacuum vessel, magnetic coils, shell, transformer limbs and concrete shielding walls (Fig.3). Outside the shell and before the walls, however, there are numerous substantial structures which have not been modeled in detail. Moreover, the vacuum vessel has ports through which neutrons may escape. These complications are approximated with a zone composed of iron, plastic and copper which has been adjusted in thickness until the JET external fission chamber measurements were consistent with the fluxes in the MCNP model. This approximation was necessary since the complexity in the torus hall is too great for more detailed modeling on a realistic timescale. The Surface Source Write file registered neutrons on a spherical surface with center at the SW Hall corner (1.0m above the floor level) and radius of 5.0m (Fig.2). The Surface Source Write file was used as Surface Source Read input file for the subsequent labyrinth calculations performed in the context of this work.

2.3 TALLIES

Neutron fluence was calculated using track length estimate tallies of neutron flux in spherical cells of 0.3 m in radius positioned along the maze at 1.0m height from the floor level. Moreover, ambient dose equivalent, H*(10), was calculated folding neutron flux by ambient dose equivalent to neutron fluence conversion factors as a function of neutron energy (ICRP, 2007). It is noted that

the ambient dose equivalent H*(10) at a point of interest in a radiation field is the dose equivalent which would be generated in the associated oriented and expanded radiation field at a depth of 10mm on the radius of the ICRU sphere which is oriented opposite to the direction of incident radiation. Statistical uncertainties were kept below 10% for all track length estimate tallies.

3. RESULTS AND DISCUSSION

3.1. NEUTRON FLUENCE ALONG THE LABYRINTH

Figures 4 and 5 show the MCNP predicted neutron energy spectrum at positions M1-M6 along the labyrinth for D-D and D-T JET plasma sources, respectively. Position M1 corresponds to the inner entrance of the labyrinth (mouth) and position M6 to the exit door.

The neutrons that are directed towards the labyrinth mouth have already been scattered by the machine, surrounding structures and wall materials one or more times and have lost a significant fraction of their kinetic energy. The mean energy of neutrons at the labyrinth mouth (M1) for the D-D and D-T source was approximately 270keV and 650keV, respectively. However, during their propagation along the labyrinth, neutrons are elastically scattered by the wall materials and are further slowed down. The mean neutron energy at labyrinth position M3 for the D-D and the D-T source was 40keV and 70keV, respectively. At the exit (M6) neutron energy was in the eV region for both sources.

Figsures 6 and 7 show the results of MCNP calculations of neutron fluence along the labyrinth, as a function of the summed centerline distance (L) from the inner labyrinth entrance (mouth) to the exit door, divided by the square root of the labyrinth cross-sectional area (A) for the D-D and D-T plasma sources, respectively. The results were normalized per JET source neutron. In these figures neutron fluence is presented in three energy groups: “thermal” (E<0.5 eV), “epithermal” (0.5 eV<E<0.1 MeV) and “fast” (E>0.1 MeV). The total neutron fluence (sum of the three groups) is also shown.

From Fig. 6 it can be seen that the total neutron fluence is attenuated along the maze (total length of 11.8 m) by about four orders of magnitude. The neutron fluence at the labyrinth exit was $(1.7 \pm 0.1)\times10^{-13}$ cm^{-2} per JET neutron. In the first two legs of the labyrinth (sections M1-M2 and M2-M3) neutron fluence is dominated by epithermal neutrons. However, for $L/A^{0.5} \geq 4.5$ the thermal neutron group becomes the dominant one. At the labyrinth mouth (M1) the relative contribution of the fast, epithermal and thermal groups to the total neutron fluence was found to be 34%, 62% and 4%, respectively. At the second right-angle bend of the labyrinth (M3) the relative contribution to neutron fluence of the fast, epithermal and thermal groups was found to be 9%, 64% and 27%, respectively. At the exit door (M6), the relative contribution of fast, epithermal and thermal groups was 1%, 15% and 84%, respectively. Since the neutron fluence at the labyrinth exit is dominated by low energy neutrons, a further attenuation of the neutron fluence can easily be achieved by using a thermal neutron absorbing material (i.e. ^{6}Li-doped polyethylene) at the door shield. A similar behavior was also observed for the D-T plasma source (Fig.7).

3.2. AMBIENT DOSE EQUIVALENT ALONG THE LABYRINTH

Fig. 8 shows the MCNP calculated ambient dose equivalent, H*(10), along the labyrinth as a function of the parameter L/A0.5 for the D-D and D-T sources. The results are normalized per JET neutron. As it can be seen, in both cases the ambient dose equivalent is decreasing along the total length of the labyrinth. The H*(10) at the labyrinth exit for the D-D and the D-T source was of $(2.0 \pm 0.2) \times 10^{-12}$ pSv and $(2.3 \pm 0.6) \times 10^{-12}$ pSv per JET neutron, respectively. The labyrinth transmission factor was found to be 1.2×10^{-5} and 1.5×10^{-5} for the D-D and the D-T source, respectively. The labyrinth transmission factor was defined as the ratio of the calculated ambient dose equivalent at the labyrinth exit (M6) over the calculated dose at the labyrinth mouth (M1) and is considered to be an index of the effectiveness of the labyrinth in attenuating streaming neutrons. The comparable calculated H*(10) values at the labyrinth exit in D-D and D-T operation modes (per JET neutron) are attributed to the fact that neutrons entering the labyrinth have already been slowed down due to multiple interactions in the Torus and wall materials and their propagation along the labyrinth has become independent of their initial energy at the point of production (source). It has to be stressed that the results shown in Fig. 8 depend on the labyrinth geometric configuration and shielding materials employed. Therefore, cannot be readily generalized to other neutron sources and labyrinth configurations as well.

3.3 EFFECT OF CONCRETE COMPOSITION

The ratio of H*(10) values calculated at the labyrinth exit for the tested concretes over the values calculated for the concretes with "as-built" composition for the D-D plasma source is shown in Fig.9. In this figure X-axis represents the alteration in hydrogen concentration in concrete in steps of 0.05% from the "as built" values of 0.56 % and 0.20% for the plain and borated concrete, respectively. The statistical errors of the calculations were below 6% for all data points. It can be seen that a decrease in hydrogen concentration in both concretes by 0.05 % results in an increase of neutron dose at the labyrinth exit of 25%. A similar result was also observed for the D-T source. In Fig. 10, the neutron fluence at the labyrinth exit is plotted as a function of boron content in the surface concrete layer (of 30 cm in thickness) for the D-D source. It can be seen that an increase in boron concentration in concrete from 0 to 1% resulted in a reduction in neutron fluence at the labyrinth exit by a factor of about 2. For a higher boron concentration the dose reduction at the labyrinth exit was small, since all slow neutrons were absorbed by the wall material. Again a similar result was observed for the D-T source.

4. VALIDATION OF RESULTS

The results of the calculations were validated by comparison against measurements using thermoluminescence detectors (TLDs). Sets of MCP-N and MCP-7 type TLDs were positioned within cylindrical polyethylene moderators in several locations in the Hall including the region of the labyrinth. The detector irradiation was carried out during JET C31 experimental campaign in

D-D operation mode. The experimental procedure and detector calibration was described in detail by Obryk et al (2014a, 2014b). Table 2 shows the comparison of the calculated and measured neutron fluence at three detector positions in the labyrinth region. Detector assembly A3 was positioned near the labyrinth mouth, detector A4 was in the middle of labyrinth section M1-M2 (1st leg) and detector A5 was at section M2-M3 (2nd leg). Calculations were normalized per 2.38×10^{18} neutrons produced at the source during the experimental campaign.

From Table 2 a systematic overestimation of the calculations over the measurements can be observed. The derived C/E values were in the range of 1.6 to 2.8. The observed discrepancy in C/E ratios was mainly attributed to approximations in the model geometry. In particular, although the JET tokamak and the labyrinth configurations were described to sufficient details in the MCNP model, the diagnostic systems, heating systems and various equipments surrounding the machine were not accurately described in the model, since a homogeneous material zone was used instead. These components have an attenuation effect on neutron fluence that is not adequately described by the model and therefore calculations overestimated the neutron fluence results.

In addition, as it was shown in section 3.3 changes in concrete composition may introduce significant errors in the neutron streaming calculations. In this work, the "as-built" concrete composition data were used. However, the uncertainties in these data and, most particularly, in H and B concentration, were not known. Nevertheless, the results shown in Figs.9 and 10 indicate that uncertainties in wall material composition cannot fully explain the observed differences in C/E ratios.

Taking into consideration the overall complexity of the modeled configuration the C/E ratios found in this study should be considered as a satisfactory agreement. Furthermore, Loughlin et al (2001) compared neutron transport calculations performed to determine neutron spectrum at a number of points in the JET torus Hall against measurements using activation detectors and they also reported discrepancies by a factor of three for reactions with little sensitivity to thermal neutrons.

5. GENERAL DISCUSSION AND CONCLUSIONS

Neutron streaming through tokamak ducts and channels has been studied by several workers (Angelone et al., 2000, Fischer et al., 2003, Sato et al., 2003, Yamauchi et al. 2005, Chen et al. 2007, Konno et al., 2007, Ochiai et al., 2007, Moro et al, 2009, Serikov et al., 2012). Nevertheless, less attention has been given to neutron streaming through larger ducts or labyrinths in the tokamak biological shield. The methodologies generally used for the calculation of neutron streaming along multi-bent large ducts in accelerator facilities include application of the Monte Carlo technique and the use of predetermined "universal" analytical expressions (Huddleston et al., 1968, Dinter et al., 1993, Mauro and Silari, 2009,). The advantage offered by the Monte Carlo simulation approach is the capability to explicitly model the source, geometry and materials configuration encountered. Nevertheless, neutron streaming through labyrinths can often be calculated to a sufficient level of

accuracy by the use of predetermined analytical expressions. Mauro and Silari (2009) compared results from Monte Carlo simulations and from analytical expressions available in the literature and concluded that universal transmission curves are applicable in many situations, in particular when the radiation source is not in direct view of the duct mouth. Preliminary calculations performed using analytical expressions (Dinter et al., 1993) provided results that were comparable with those calculated in the present study using the MCNP code only for the third and fourth labyrinth legs, where no borated concrete was used at the walls and neutrons were predominantly in the thermal energy region. For the first and second legs, however, the analytical expressions could not be applied since they could not account for the borated concrete surface layers and therefore significantly overestimated the results of neutron streaming.

The similar neutron transmission values obtained for the D-D and the D-T JET plasma discharge sources were attributed to the fact that neutrons have been slowed down due to multiple interactions with the Torus and wall material and their propagation along the labyrinth has become independent of the initial energy of the neutron source and depend only on the labyrinth geometry and material configuration. Elastic neutron scattering in hydrogen and slow neutron absorption in boron in concrete have a significant effect on neutron streaming. Therefore, the results of this study showed that the accuracy of the neutron streaming simulations through the JET labyrinth depends on the exact knowledge of the labyrinth geometry and wall composition and is practically independent of the source neutron spectrum.

The calculations were validated by comparison against experimental measurements carried out using thermoluminesance detectors. The results of the comparison showed that the calculations overestimated the fluence by a factor of up to 3 in the labyrinth region. The C/E discrepancy was mainly attributed to approximations in the geometry model and in particular on the approximations used to describe the instruments and facilities surrounding the tokamak which was not possible to be modeled in detail in a realistic timescale. Nevertheless, the C/E ratios found in this study are considered as in a satisfactory agreement taking into consideration the overall complexity of the JET tokamak and shielding configuration studied. New experiments are in progress and a detailed comparison of calculated and experimental values will be performed aiming to obtain a full validation of the presented analysis. The detectors will be exposed to significantly higher neutron fluence in order to obtain experimental data with improved uncertainties along the total length of the labyrinth. This work discussed Monte Carlo simulations performed using the MCNP code to calculate neutron streaming along the JET Hall SW personnel entrance labyrinth. Neutron fluence and ambient dose equivalent were calculated along the length of the labyrinth. The results of the present work primarily support the continuous operational radiation protection effort to minimize collective radiation dose to JET personnel during the D-D and the now under preparation D-T experimental campaigns. Moreover, they provide important information from JET experience that may assist in optimizing and validating the large duct and labyrinth radiation shielding design methodology used in ITER.

ACKNOWLEDGMENTS

This work was supported by EURATOM and carried out within the framework of the European Fusion Development Agreement (EFDA), under JET Fusion Technology task JW13-FT-5.48. The views and opinions expressed herein do not necessarily reflect those of the European Commission.

REFERENCES

[1]. Aldama, D.L., Trkov, A., 2004, FENDL-2.1: Evaluated nuclear data library for fusion applications, INDC(NDS)-467.

[2]. Angelone, M., Batistoni, P., Petrizzi, L., Pillon, M., 2000, Neutron streaming experiment at FNG: results and analysis, Fus. Eng. Des., 51–52, 653-661.

[3]. Batistoni, P., Likonen, J., Bekris, N., Brezinsek, S., Coad, P., Horton, L., Matthews, G., Rubel, M., Sips, G., Syme, B., Widdowson, A., 2014, The JET technology program in support of ITER, Fus. Eng. Des., article in press, DOI: 10.1016/j.fusengdes.2013.12.050.

[4]. Chen, Y., Fischer, U., Simakov, S.P., Wasastjern, F., 2007, Shielding analyses of the IFMIF test cell, J. Nucl. Mater. 367–370, 1580-1585.

[5]. Dinter, H., Dworak, D. and Tesch, K., 1993, Attenuation of the neutron dose equivalent in labyrinths through an accelerator shield, Nucl. Instr. Meth. Phys. Res. A, 333, 507-512.

[6]. Gatu Johnson, M., Giacomelli, L., Hjalmarsson, A., Källne, J., Weiszflog, M., Andersson Sundén, E., Conroy, S., et al., 2008, The 2.5-MeV neutron time-of-flight spectrometer TOFOR for experiments at JET, Nucl. Instr. Meth. A, 591, 417-430.

[7]. Huddleston, C.M., LeDoux, J. C., Burrus, W. R., Bergelson, B. R., Mashkovich, V. P., Aalto, E., Nilsson, J., Sandlin, R., Vesely, W. E., Maerker, R. E., Claiborne, H. C., Clifford, C. E., 1968, Ducts and Voids in Shields, in Engineering Compendium on Radiation Shielding, Vol. I: Shielding Fundamentals and Methods, Ed. Jaeger R.G. et al., Springer-Verlag, Berlin, 1968, 487-530.

[8]. International Commission on Radiological Protection (ICRP), 2007, The 2007 Recommendations of the International Commission on Radiological Protection, Publication 103, Ann. ICRP 37 (2-4) 2007.

[9]. Konno, C., Maekawa, F., Uno, Y., Kasugai, Y., Wada, M., Ikeda, Y., Takeuchi, H., 2000, Overview of straight duct streaming experiments for ITER, Fus. Eng. Des., 51–52, 797-802.

[10]. Loughlin, M.J., Forrest, R.A., Edwards, J.E.G., 2001 Neutron Activation Studies on JET, Fus. Eng. Des., 58–59, 967–971.

[11]. Mauro, E., Silari, M., 2009, Attenuation of neutrons through ducts and labyrinths, Nucl. Instr. Meth. Phys. Res. A, 608, 28-36.

[12]. McKinney, W.G., et al., 2006, MCNPX overview, Proceedings of the 2006 HSSW, FNAL, IL, LA-UR-06-6206. Sept. 2006.

[13]. Moro, F., Petrizzi, L., Brolatti, G., Esposito, B., Marocco, D., Villari, R., 2009, The ITER radial neutron camera: An updated neutronic analysis, Fus. Eng. Des., 84, 1351-1356.

[14]. Obryk, B., Batistoni, P., Conroy, S., Syme, B.D., Popovichev S., Stamatelatos, I.E., Vasilopoulou, T., Bilski, P., 2014, Thermoluminescence measurements of neutron streaming through JET Torus Hall ducts, Fus. Eng. Des., article in press, DOI: 10.1016j.fusengdes.2013.12.045.

[15]. Obryk, B., Stamatelatos, I.E., Vasilopoulou, T., Batistoni, P., Conroy, S., Popovichev, S., Syme D.B., 2014, Measurements and analysis of neutron streaming through JET Torus hall ducts, WP13-FT-5.48, Report to EFDA JET Fusion Technology Program

[16]. Ochiai, K., Sato, S., Wada, M., Kubota, N., Kondo, K., Yamauchi, M., Abe, Y., Nishitani, T., Konno, C., 2007, Thin slit streaming experiment for ITER by using D-T neutron source, Fusion Eng. Des., 82, 2794-2798.

[17]. Santamarina, A., Bernard, D., Blaise, P., Coste, M., Courcelle, A., Huynh, T.D., Jouanne, C., Leconte, P., Litaize, O., Mengelle, S., Noguère, G., Ruggiéri, J-M., Sérot, O., Tommasi, J., Vaglio, C., Vidal J-F., 2009, The JEFF-3.1.1 Nuclear Data Library, JEFF Report 22, NEA No. 6807, OECD, ISBN 978-92-64-99074-6.

[18]. Sato, S., Maki, K., 2003, Analytical representation for neutron streaming through slits in fusion reactor blanket by Monte Carlo calculation, Fus. Eng. Des., 65, 501-524.

[19]. Serikov, A., Fischer, U., Leichtle, D., Pitcher, C.S., 2012, Monte Carlo radiation shielding and activation analyses for the Diagnostic Equatorial Port Plug in ITER, Fusion Eng. Des. 87, 690-694.

[20]. Yamauchi, M., Ochiai, K., Morimoto, Y., Wada, M., Sato, S., Nishitani, T., 2005, Experiment and analyses for 14 MeV neutron streaming through a dogleg duct, Radiat. Prot. Dosim., 116, 542-546.

Element or Isotope	Weight Fraction	
	Plain	Borated
Al	0.8	6.5
Ba	0.026	0.045
B-10	0.0008	0.14
B-11	0.0032	0.56
Ca	28	6.5
C	7.9	0.18
Cr-50	0.000129	0.000103
Cr-52	0.002514	0.002011
Cr-53	0.000285	0.000228
Cr-54	0.0000709	0.000057
Co	0.00066	0.0008
Cu-63	0.0005533	0.001522
Cu-65	0.0002466	0.000678
Eu-151	0.0000239	0.000033
Eu-153	0.0000261	0.000037
Ga	0.0004	0.0016
H	0.56	0.2
Fe-54	0.1508	0.174
Fe-56	2.38472	2.752
Fe-57	0.052	0.06
Fe-58	0.00728	0.0084
Mg	0.55	0.8
Mn	0.04	0.05
O	47.9	47.4
K	0.3	1.4
Si	12	29.6
Na	0.035	1.6
S	0.18	0.13
Ti	0.035	0.45
Th	0.00022	-
Zn	0.003	-

Table 1 Concrete compositions used in the present study ("as-built")

Detector	Fluence ($cm^{-2} n^{-1}$)		C/E ratio
	Calculated	Experimental	
A3	1.68E+09 (4.8)	1.03E+09 (12.7)	1.62 (13.6)
A4	9.63E+08 (4.1)	3.86E+08 (18.0)	2.49 (18.4)
A5	5.64E+07 (8.8)	2.01E+07 (17.7)	2.81 (19.8)

Table 2 Comparison of calculated and measured neutron fluence at three labyrinth positions (with their % relative errors).

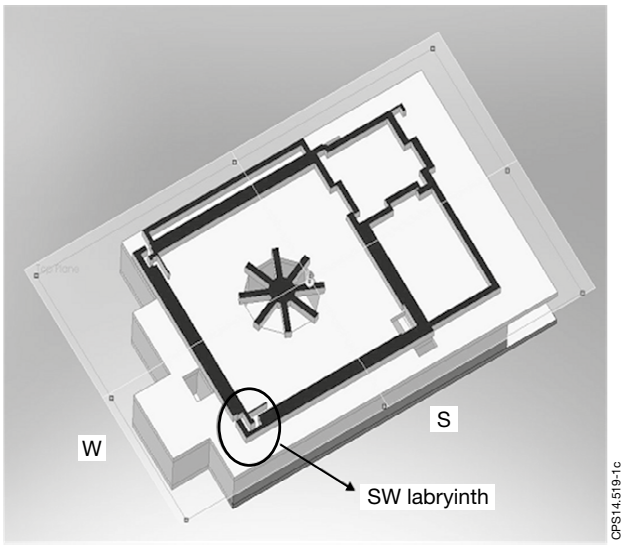

Figure 1: Ground view of JET Hall showing the location of the SW personnel entrance labyrinth.

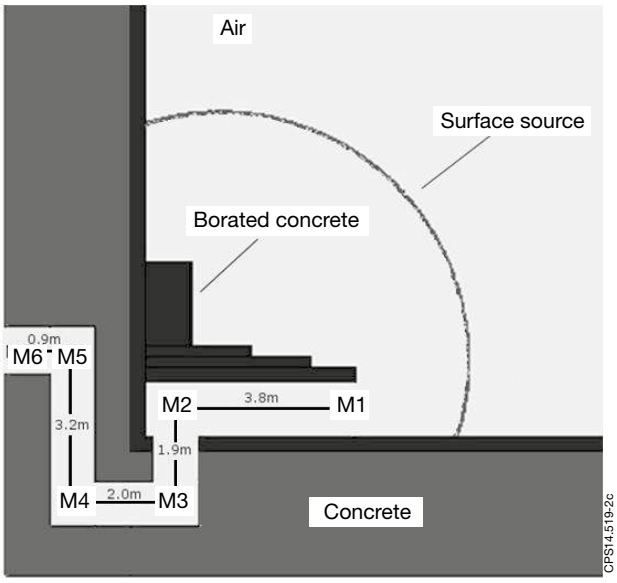

Figure 2: Cross sectional view of the SW entrance labyrinth.

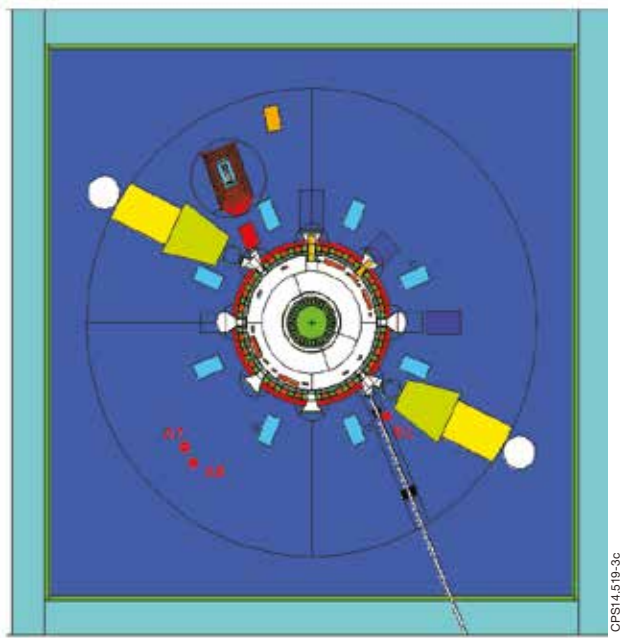

Figure 3: MCNP model of JET (cross section on the machine mid-plane).

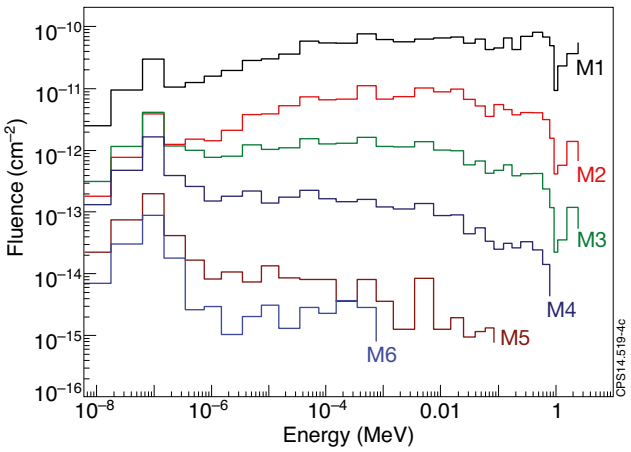

Figure 4: Neutron energy spectrum at labyrinth positions M1-M6 for the D-D source.

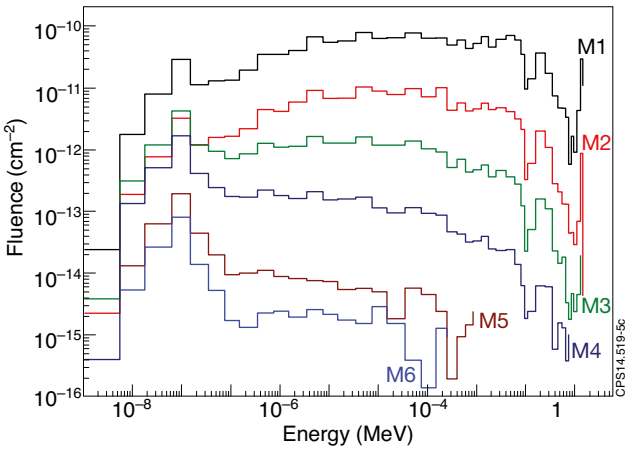

Figure 5: Neutron energy spectrum at labyrinth positions M1-M6 for the D-T source.

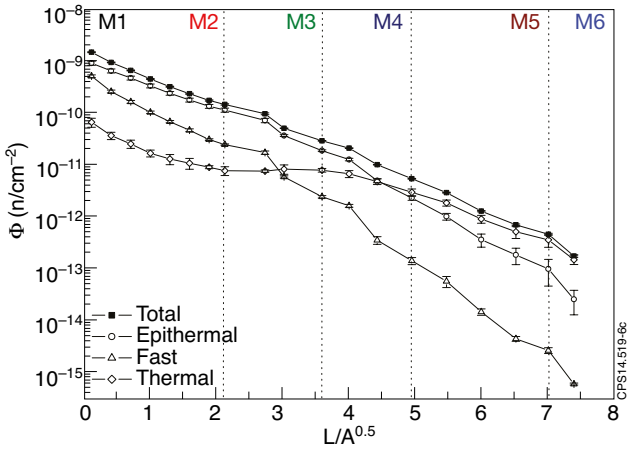

Figure 6: Neutron fluence as a function of parameter L/A0.5 for D-D plasma source (normalization per JET neutron).

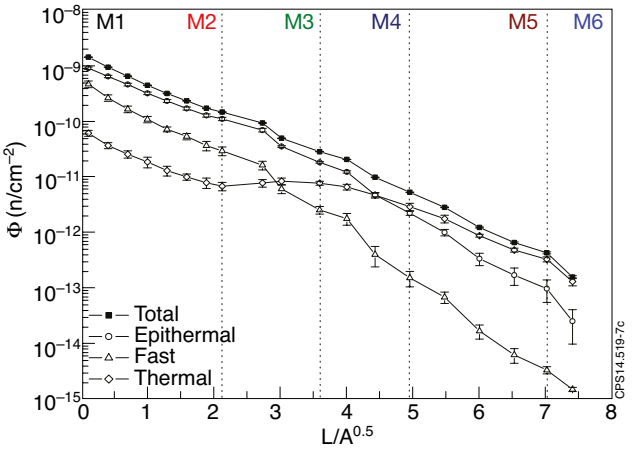

Figure 7: Neutron fluence as a function of parameter L/A0.5 for D-T plasma source (normalization per JET neutron).

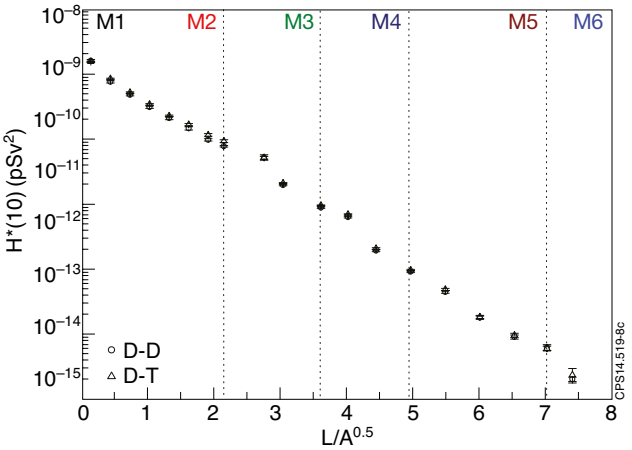

Figure 8: Neutron ambient dose equivalent, H(10), as a function of L/A0.5 for D-D and D-T plasma sources (per JET neutron).*

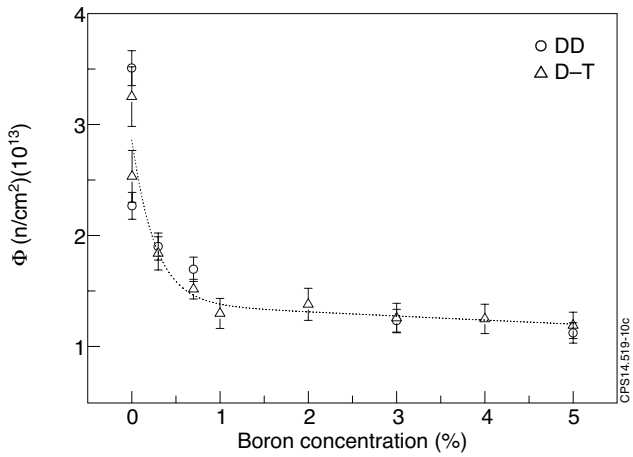

Figure 9: MCNP calculated neutron ambient dose equivalent, H(10) at the labyrinth exit as a function of difference in H concentration in concrete.*

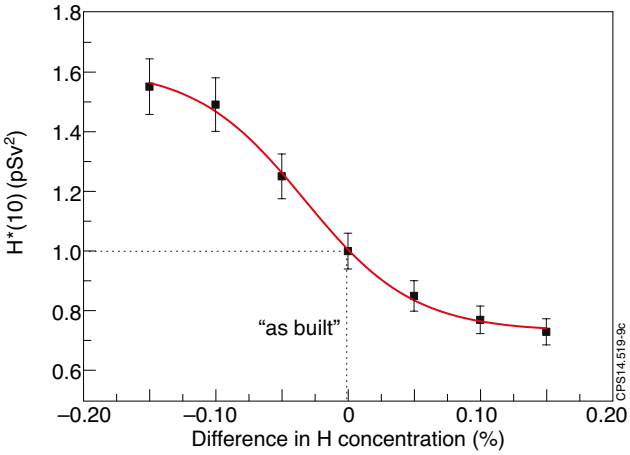

Figure 10: MCNP calculated neutron fluence at the labyrinth exit as a function of boron concentration in concrete for D-D and D-T plasma sources.